14th International Conference on Structural Safety and Reliability - ICOSSAR'25
1-6 June, 2025 - Los Angeles California, USA
R. Ghanem, E. Johnson, S. Masri and A. Olivier (Eds)

AN APPROXIMATE ANALYTICAL METHOD FOR EVALUATING THE FIRST-CROSSING PROBABILITY OF BASE-ISOLATED STRUCTURES SUBJECTED TO STOCHASTIC PULSE-LIKE GROUND MOTIONS

Renjie Han[1,2,3,4], Robby Caspeele[3], Yongbo Peng[1], Mia Loccufier[4], Xin Zhao[2,5]

[1] State Key Laboratory of Disaster Reduction in Civil Engineering, Tongji University, Shanghai 200092, China

[2] College of Civil Engineering, Tongji University, Shanghai 200092, China

[3] Department of Structural Engineering and Building Materials, Ghent University, Ghent 9000, Belgium

[4] Department of Electromechanical, Systems and Metal Engineering, Ghent University, Ghent 9000, Belgium
[5] Tongji Architectural Design (Group) Co., Ltd, Shanghai 200092, China

Key words: pulse-like ground motion, base-isolated structures, non-zero-mean response, first-passage reliability, Bouc-Wen systems

Abstract. This study presents an efficient method for evaluating the first-crossing probability of base-isolated structures (BIS) subjected to stochastic pulse-like ground motions (PLGMs), with emphasis on the inherent randomness of the excitation. First, the PLGMs are modeled as non-zero-mean random processes, consisting of a deterministic pulse component and a stochastic component characterized by its power spectral density. Consequently, the corresponding stochastic structural response also exhibits a non-zero mean and is approximated using a novel analytical approach, termed SLT-RKA (statistical linearization technique combined with the Runge-Kutta algorithm). Subsequently, a generalized closed-form expression for the decay rates is derived to account for the time-varying mean of the response. Finally, the decay rates are utilized to estimate the first-crossing probability based on the Poisson out-crossing assumption. The accuracy and computational efficiency of the proposed method are validated through comparisons with Monte Carlo simulation (MCS) results in representative numerical examples.

1 Introduction

Over the past decades, base-isolated structures (BIS) have demonstrated considerable effectiveness in mitigating the seismic response of superstructures during strong earthquake events [1]. As a result, BIS have been widely implemented in critical infrastructure such as high-rise buildings, hospitals, nuclear facilities, industrial plants, and data centers [2]. However, for structures subjected to near-fault pulse-like ground motions (PLGMs), the performance of base isolation may be significantly compromised [3], raising serious concerns about its reliability in such scenarios.

PLGMs, typically characterized by velocity pulses arising from forward directivity or fling-step effects [4, 5], have been consistently shown to cause more severe structural damage compared to ordinary ground motions. This heightened destructiveness has motivated extensive research on modeling PLGMs. Existing models include deterministic formulations, wavelet-based representations [6], enhanced parameterization techniques, and stochastic parameter distributions [7]. Among these, hybrid models—where PLGMs are decomposed into a deterministic pulse component and a stochastic residual component modeled using power spectral density (PSD) functions—have gained prominence [8, 9, 10].

In particular, the stochastic modeling of PLGMs poses unique challenges. Traditional ground motion models based on PSD typically assume ground motions to be zero-mean random processes [11, 12]. However, the presence of a deterministic pulse component leads to a non-zero-mean, time-varying excitation process, rendering many well-established analytical random vibration methods inapplicable. Although simulation-based approaches, such as Monte Carlo simulations (MCS), remain viable [2], they are computationally intensive and thus impractical for engineering applications.

Given the significant impact of PLGMs on BIS and the distinct modeling approach they require, there is a clear need for an efficient method for reliability analysis. To address this, the proposed method combines statistical linearization, the Runge-Kutta algorithm, and the probabilistic out-crossing theory. Specifically, the PLGM is modeled as a non-zero-mean random process composed of a deterministic pulse component and a stochastic residual characterized by its PSD. The corresponding structural response, which also exhibits a non-zero mean, is approximated analytically using a statistical linearization technique combined with the Runge-Kutta algorithm (SLT-RKA) [13]. A generalized closed-form expression for the response decay rate is then derived to account for the time-varying mean, enabling the estimation of the first-crossing probability within a Poisson out-crossing framework [14]. The proposed method demonstrates both high accuracy and computational efficiency, as verified through comparisons with Monte Carlo simulation (MCS) results in representative numerical examples. This makes it a practical and efficient tool for performance-based seismic design of base-isolated structures subjected to near-fault PLGMs.

2 Stochastic Modeling of Pulse-Like Ground Motions

To establish a reliability analysis framework for BIS under PLGMs, it is necessary to first develop a suitable stochastic model that captures both the pulse and random features of PLGMs.

PLGMs are typically decomposed into two distinct components: a dominant pulse component and a residual component that accounts for the remaining stochastic content. This decomposition is expressed as

$$\ddot{x}_g(t) = \ddot{x}_p(t) + \ddot{x}_r(t), \tag{1}$$

where $\ddot{x}_p(t)$ is interpreted as the deterministic pulse component, and $\ddot{x}_r(t)$ represents the zero-mean residual component, which is modeled using a PSD model. The estimation and modeling of these two components are presented in the following sebsections.

2.1 Pulse Component: Extraction and Formulation

The extraction of the actual pulse component from recorded PLGMs is conducted using the wavelet-based approach proposed by Baker [4]. This procedure is applied to the velocity time history of the ground motion, where the wavelet transform is performed iteratively ten times to identify the wavelet with the largest coefficient. The extracted pulse velocity is denoted as $\hat{\dot{x}}_p(t)$.

The pulse velocity is then modeled using a wavelet-based functional form [9]:

$$\dot{x}_p(t) = V_p \cdot \exp\left[-\frac{\pi^2}{4}\left(\frac{t-T_{pk}}{N_c T_v}\right)^2\right] \cdot \cos\left(2\pi\frac{t-T_{pk}}{T_v} - \varphi\right), \tag{2}$$

where V_p, T_v, N_c, T_{pk}, and φ denote the peak pulse velocity, velocity period, number of periods, pulse occurrence time and phase, respectively, identified by minimizing the mean squared error between the model and the extracted pulse velocity $\hat{\dot{x}}_p(t)$.

Subsequently, the corresponding pulse acceleration is obtained by differentiating Eq. (2), as presented in [13].

$$\begin{aligned}\ddot{x}_p(t) = &-\frac{V_p \pi^2 (t-T_{pk})}{2(N_c T_v)^2} \cdot \exp\left[-\frac{\pi^2}{4}\left(\frac{t-T_{pk}}{N_c T_v}\right)^2\right] \cdot \cos\left(2\pi\frac{t-T_{pk}}{T_v} - \varphi\right) \\ &- \frac{2V_p\pi}{T_v} \cdot \exp\left[-\frac{\pi^2}{4}\left(\frac{t-T_{pk}}{N_c T_v}\right)^2\right] \cdot \sin\left(2\pi\frac{t-T_{pk}}{T_v} - \varphi\right).\end{aligned} \tag{3}$$

2.2 Residual Component: Power Spectral Density Model and Estimation

The residual component $\hat{\ddot{x}}_r(t)$ is obtained by removing the extracted pulse component from the original ground motion and is considered a realization of a zero-mean random process. To model this component, a power spectral density (PSD) function is employed, targeting the estimated spectrum $\hat{S}(\omega)$, which is computed using the multi-taper method [15]. This approach enhances the robustness of the spectral estimate by reducing variance and minimizing spectral leakage.

In this study, the Clough–Penzien model [16] is adopted as the power spectral density (PSD) model:

$$S_{C-P}(\omega) = \frac{1 + 4\xi_g^2\left(\frac{\omega}{\omega_g}\right)^2}{\left[1-\left(\frac{\omega}{\omega_g}\right)^2\right]^2 + 4\xi_g^2\left(\frac{\omega}{\omega_g}\right)^2} \cdot \frac{\left(\frac{\omega}{\omega_f}\right)^4}{\left[1-\left(\frac{\omega}{\omega_f}\right)^2\right]^2 + 4\xi_f^2\left(\frac{\omega}{\omega_f}\right)^2} \cdot S_0. \tag{4}$$

The model parameters in Eq. (4) are calibrated to fit the estimated spectrum $\hat{S}(\omega)$ using the minimum mean square error method. Here, ω_g and ξ_g denote the natural frequency and damping ratio of the ground filter, respectively; ω_f and ξ_f represent the natural frequency and damping ratio of the high-frequency filter, respectively; and S_0 is the intensity parameter characterizing the overall magnitude of the power spectral density. The Clough-Penzien PSD originates from a zero-mean white noise random process $w\left(t\right)$ with intensity S_0 passing through a two-stage filter system, expressed as follows [17]:

$$\ddot{x}_r\left(t\right) + 2\xi_g\omega_g\dot{x}_r\left(t\right) + \omega_g^2 x_r\left(t\right) = -\left[\ddot{x}_f\left(t\right) + w\left(t\right)\right], \tag{5}$$

$$\ddot{x}_f\left(t\right) + 2\xi_f\omega_f\dot{x}_f\left(t\right) + \omega_f^2 x_f\left(t\right) = -w\left(t\right), \tag{6}$$

where $x_f(t)$ denotes the in intermediate response of the high-frequency filter.

2.3 Amplitude Modulation: Formulation and Normalization

To capture the time-varying intensity of the residual component, its envelope also needs to be modeled. The estimated envelope $\hat{A}(t)$ of the residual acceleration is derived using Dugundji's envelope [18], computed via the Hilbert transform of the acceleration time history:

$$\hat{A}(t) = \sqrt{\ddot{x}_g^2(t) + \tilde{\ddot{x}}_g^2(t)}, \tag{7}$$

where $\tilde{\ddot{x}}_g(t)$ denotes the Hilbert transform of $\ddot{x}_g(t)$.

The classical exponential amplitude modulation function is employed to represent the intensity non-stationarity of $\ddot{x}_g(t)$:

$$E(t) = H \cdot [\exp(-\mu_1 t) - \exp(-\mu_2 t)], \tag{8}$$

where μ_1 and μ_2 are the decay rates, and H is the intensity parameter. The modulation function parameters are first estimated by fitting to the envelope $\hat{A}(t)$, and then the function is normalized so that its peak value equals 1.

Accordingly, the final PSD model $S(\omega, t)$ for the residual component is expressed as:

$$S(\omega, t) = E^2(t) \cdot S_{C-P}(\omega). \tag{9}$$

2.4 Summary and Implementation

For the modeling process, the time step is uniformly set to 0.02 s, and the time histories are truncated between 0.1% and 99.8% of the cumulative energy to normalize the duration. A pulse-like ground motion downloaded from the NGA-West2 database (denoted as Sample 1) is used to demonstrate the modeling procedure. This ground motion has been classified as a pulse-like record with dominant pulse characteristics, as identified in [5]. A detailed summary of all fitted model parameters is provided in Table 1, and the modeling results are illustrated in Figs. 1(a)–1(c), confirming that the proposed method effectively captures the essential features of PLGMs, including the long-period pulse, spectral content, and non-stationary intensity variation.

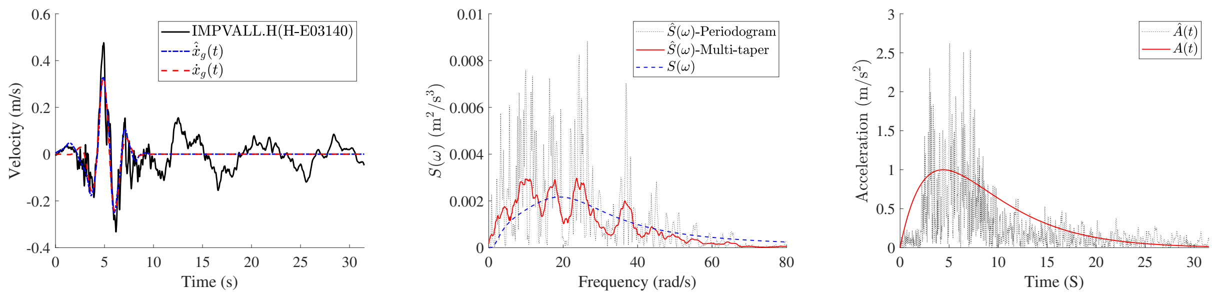

(a) (b) (c)

Figure 1: Models for (a) pulse-component, (b) power spectral density, and (c) envelope.

Table 1: Model parameters of Sample 1: IMPVALL.H(H-E03140)

Model parameter	V_p (m/s)	T_{pk} (s)	N_c	T_v (s)	ϕ	H
Identified value	0.33	5.13	1.06	2.57	-0.65	27.11
μ_1	μ_2	S_0 (10^{-3} m^2/s^3)	ξ_g	ω_g (rad/s)	ξ_f	ω_f (rad/s)
0.22	0.24	1.40	0.70	23.62	1.00	2.36

3 Reliabilty analysis for BIS subjected to PLGMs

Since the base-isolation system mitigates the transmission of ground motion effects to the superstructure, the superstructure can be reasonably assumed to behave as a rigid body, while the base isolation layer exhibits hysteretic nonlinear behavior. Accordingly, the BIS can be modeled as a single-degree-of-freedom (SDOF) system governed by the Bouc-Wen hysteresis model [19]. The equation of motion for the BIS subjected to PLGM is given by

$$m\ddot{x} + c\dot{x} + \alpha kx + (1-\alpha)F_y z = -m\ddot{x}_g(t), \tag{10}$$

where x, $\dot{x}$, and $\ddot{x}$ denote the displacement, velocity, and acceleration responses of the BIS, respectively. The variable z represents the hysteretic displacement, which evolves according to the nonlinear differential equation

$$\dot{z} = \frac{A\dot{x} - \gamma|\dot{x}|z - \beta\dot{x}|z|}{x_y}, \tag{11}$$

where x_y is the yield displacement of the isolation layer, and A, γ, and β are model parameters that define the shape and characteristics of the hysteresis loop. The parameters m, c, and k represent the mass, damping coefficient, and pre-yield stiffness of the system, respectively. The parameter α denotes the ratio of post-yield stiffness to pre-yield stiffness, and the yielding strength F_y is given by $F_y = kx_y$. The excitation $\ddot{x}_g(t)$ denotes the stochastic pulse-like ground motion, modeled as described in Section 2.

3.1 Stochastic response of the BIS subjected to PLGMs

The stochastic response of Eq. (10) is characterized as a random process with a time-varying mean. For instance, the response can be expressed as

$$x = \mu_x + s_x, \quad \dot{x} = \mu_{\dot{x}} + s_{\dot{x}}, \quad z = \mu_z + s_z, \tag{12}$$

where μ_x, $\mu_{\dot{x}}$, and μ_z denote the mean components, and s_x, $s_{\dot{x}}$, and s_z represent the corresponding zero-mean stochastic components.

The response can be approximated using the SLT-RKA (statistical linearization technique and Runge-Kutta algorithm) method [13]. The core idea of this method is to decouple the deterministic and stochastic parts of the response and to solve the resulting set of coupled differential equations using a state-space formulation combined with the Lyapunov equation. The covariance matrix of the stochastic component is computed by solving the Lyapunov equation via statistical linearization. The entire system of differential equations is then solved simultaneously using the Runge-Kutta method. Detailed descriptions of the SLT-RKA method are provided in Ref. [13].

Applying the SLT-RKA method, the governing equations for the mean response components, defined as $\mathbf{p} = [p_1, p_2, p_3]^{\mathrm{T}} = [\mu_x, \mu_{\dot{x}}, \mu_z]^{\mathrm{T}}$, can be written as

$$\dot{p}_1 = p_2, \tag{13}$$

$$\dot{p}_2 = -\ddot{x}_g(t) - \frac{c}{m}p_2 - \frac{\alpha k}{m}p_1 - \frac{(1-\alpha)F_y}{m}p_3, \tag{14}$$

$$\dot{p}_3 = \frac{Ap_2 - \gamma\mathbb{E}\left[|\dot{x}|z\right] - \beta\mathbb{E}\left[\dot{x}|z|\right]}{x_y}. \tag{15}$$

The expectations in Eq. (15) can be expressed in closed form under the assumption that the response variables follow a Gaussian distribution. For instance,

$$\mathbb{E}[|\dot{x}|z] = \operatorname{erf}\left(\frac{\mu_{\dot{x}}}{\sqrt{2}\sigma_{\dot{x}}}\right)(\rho\sigma_{\dot{x}}\sigma_z + \mu_{\dot{x}}\mu_z) + \sqrt{\frac{2}{\pi}}\mu_z\sigma_{\dot{x}}\exp\left(-\frac{\mu_{\dot{x}}^2}{2\sigma_{\dot{x}}^2}\right), \tag{16}$$

where ρ is the correlation coefficient of $\dot{x}$ and z. From Eqs. (13)-(15), it is noted that, in addition to the state variables contained in $\mathbf{p}$, there exist unknown variables arising from the mathematical expectation operations. Specifically, these variables are $\sigma_{\dot{x}}$, σ_z, and ρ in the present work, which need to be determined by solving the stochastic differential equations governing the zero-mean stochastic components.

Using the statistical linearization technique, the nonlinear equation governing s_z can be approximated by an equivalent linear form that minimizes the mean-square error [13]:

$$s_{\dot{z}} = -k_e s_z - c_e s_{\dot{x}}, \tag{17}$$

where the equivalent linear coefficients k_e and c_e are given by

$$k_e = \frac{\gamma\mathbb{E}[|\dot{x}|] + \beta\mathbb{E}[\dot{x}\ \operatorname{sgn}(z)]}{x_y}, \tag{18}$$

$$c_e = \frac{-A + \gamma\mathbb{E}[z\ \operatorname{sgn}(\dot{x})] + \beta\mathbb{E}[|z|]}{x_y}. \tag{19}$$

The relevant expectations in Eqs. (18)–(19) can also be expressed in closed form as follows:

$$\mathbb{E}[\dot{x}\ \operatorname{sgn}(z)] = \sqrt{\frac{2}{\pi}}\sigma_{\dot{x}}\rho\exp\left(-\frac{\mu_z^2}{2\sigma_z^2}\right) + \mu_{\dot{x}}\operatorname{erf}\left(\frac{\mu_z}{\sqrt{2}\sigma_z}\right), \tag{20}$$

$$\mathbb{E}[|\dot{x}|] = \sqrt{\frac{2}{\pi}}\sigma_{\dot{x}}\exp\left(-\frac{\mu_{\dot{x}}^2}{2\sigma_{\dot{x}}^2}\right) + \mu_{\dot{x}}\operatorname{erf}\left(\frac{\mu_{\dot{x}}}{\sqrt{2}\sigma_{\dot{x}}}\right). \tag{21}$$

Modeling the residual ground motion component using the Clough–Penzien spectrum and treating it as filtered white noise (see Eqs. (5)–(6)) leads to the following state-space vector:

$$\mathbf{q} = [s_x, s_{\dot{x}}, s_z, x_f, \dot{x}_f, x_r, \dot{x}_r]^{\mathrm{T}}. \tag{22}$$

Accordingly, the stochastic differential equation governing the system becomes

$$\dot{\mathbf{q}} = \mathbf{G}\mathbf{q} + \mathbf{Q}w(t), \tag{23}$$

where $w(t)$ denotes white noise excitation with power spectrum density S_0,

$$\mathbf{G} = \begin{bmatrix} 0 & 1 & 0 & 0 & 0 & 0 & 0 \\ -\frac{\alpha k}{m} & -\frac{c}{m} & \frac{(\alpha-1)F_y}{m} & -\frac{E(t)\omega_f^2}{m} & -\frac{2E(t)\xi_f\omega_f}{m} & \frac{E(t)\omega_g^2}{m} & \frac{2E(t)\xi_g\omega_g}{m} \\ 0 & -c_e & -k_e & 0 & 0 & 0 & 0 \\ 0 & 0 & 0 & 0 & 1 & 0 & 0 \\ 0 & 0 & 0 & -\omega_f^2 & -2\xi_f\omega_f & \omega_g^2 & 2\xi_g\omega_g \\ 0 & 0 & 0 & 0 & 0 & 0 & 1 \\ 0 & 0 & 0 & 0 & 0 & -\omega_g^2 & -2\xi_g\omega_g \end{bmatrix}, \mathbf{Q} = \begin{Bmatrix} 0 \\ 0 \\ 0 \\ 0 \\ 0 \\ 0 \\ 1 \end{Bmatrix}. \tag{24}$$

The time evolution of the covariance matrix $\mathbf{\Gamma}$ is described by the Lyapunov equation corresponding to Eq. (23).

$$\dot{\mathbf{\Gamma}} = \mathbf{G}\mathbf{\Gamma}^{\mathrm{T}} + \mathbf{\Gamma}\mathbf{G}^{\mathrm{T}} + \mathbf{Q}D\mathbf{Q}^{\mathrm{T}}, \tag{25}$$

with $D = 2\pi S_0$ denoting the spectral intensity.

The unknown terms in Eqs. (13)–(15), namely $\sigma_{\dot{x}}$, σ_z, and ρ, are functions of the covariance matrix $\mathbf{\Gamma}$, expressed as

$$\sigma_{\dot{x}} = \sqrt{\Gamma_{2,2}}, \sigma_z = \sqrt{\Gamma_{3,3}}, \rho = \frac{\Gamma_{2,3}}{\sqrt{\Gamma_{2,2} \cdot \Gamma_{3,3}}}. \tag{26}$$

By simultaneously solving Eq. (25) and Eqs. (13)–(15) using the Runge–Kutta method, the complete stochastic response of the system can be obtained.

3.2 Reliability of the BIS subjected to PLGMs

Once the stochastic response of the system is obtained, the first-passage reliability $L(t, b)$ can be evaluated. This reliability is defined as the probability that the displacement of the BIS remains within the design limit b throughout the time interval $[0, t]$, that is,

$$L(t, b) = P\left[|x(\tau)| < b,\ 0 \leq \tau \leq t\right]. \tag{27}$$

Accordingly, when the duration of ground motion is T, the first-passage reliability over the entire excitation period becomes

$$R_b = L(T, b). \tag{28}$$

To efficiently compute the reliability, the out-crossing theory [20] is adopted. However, the classical formulation assumes a zero-mean response, which is not applicable in this study since the BIS response to PLGMs exhibits a non-zero mean in both displacement and velocity. Therefore, a generalized version of the theory is required. Assuming the out-crossing process follows a Poisson distribution, the first-passage reliability in Eq. (27) can be reformulated as

$$L(t, b) = \exp\left[-\int_0^t \lambda(\tau)\, d\tau\right], \tag{29}$$

where $\lambda(\tau)$ is the time-dependent out-crossing rate. This expression follows the classical exponential decay form of first-passage reliability [14, 20].

The formulation in Eq. (27) corresponds to a double-barrier (D-barrier) crossing problem [14]. When the barrier level is high, the out-crossing rate $\lambda(t)$ can be approximated as

$$\lambda(t) = v_x^+(t, b) + v_x^-(t, -b), \tag{30}$$

where $v_x^+(t, b)$ denotes the up-crossing rate of the upper threshold with positive slope, and $v_x^-(t, -b)$ denotes the down-crossing rate of the lower threshold with negative slope.

In contrast to the classical case, where symmetry between the up-crossing and down-crossing rates is assumed, the presence of non-zero means in both displacement and velocity leads to asymmetric crossing behaviors. Therefore, more accurate formulations of v_x^+ and v_x^- are necessary. According to Rice's formula [21], the expected crossing rates are given by

$$v_x^+(t, b) = \int_0^{+\infty} \dot{x}\, p(b, \dot{x}, t)\, d\dot{x}, \tag{31}$$

$$v_x^-(t,-b) = \int_{-\infty}^{0} (-\dot{x})\, p(-b,\dot{x},t)\, d\dot{x}, \tag{32}$$

where $p(x,\dot{x},t)$ is the joint probability density function of $x(t)$ and $\dot{x}(t)$.

Assuming $x(t)$ and $\dot{x}(t)$ are jointly Gaussian, their joint density function is expressed as

$$p(x,\dot{x}) = \frac{1}{2\pi\sigma_x\sigma_{\dot{x}}\sqrt{1-\rho_{x\dot{x}}^2}} \exp\left\{-\frac{1}{2(1-\rho_{x\dot{x}}^2)}\left[\frac{(x-\mu_x)^2}{\sigma_x^2} - \frac{2\rho_{x\dot{x}}(x-\mu_x)(\dot{x}-\mu_{\dot{x}})}{\sigma_x\sigma_{\dot{x}}} + \frac{(\dot{x}-\mu_{\dot{x}})^2}{\sigma_{\dot{x}}^2}\right]\right\}, \tag{33}$$

where all variables are determined in Section 3.1, and $\rho_{x\dot{x}}$ denotes the correlation coefficient between x and $\dot{x}$, obtained from the covariance matrix $\mathbf{\Gamma}$ as $\rho_{x\dot{x}} = \Gamma_{1,2}/\sqrt{\Gamma_{1,1}\cdot\Gamma_{2,2}}$. Based on the above assumptions, analytical expressions for the up- and down-crossing rates can be derived. The up-crossing rate is given by

$$v_x^+(t,b) = \frac{1}{\sqrt{2\pi}\sigma_x}\exp\left[-\frac{(b-\mu_x)^2}{2\sigma_x^2}\right]\cdot\left[\frac{\sigma_y}{\sqrt{2\pi}}\exp\left(-\frac{\mu_y^2}{2\sigma_y^2}\right) + \frac{\mu_y}{2}\left(\operatorname{erf}\left(\frac{\mu_y}{\sqrt{2}\sigma_y}\right)+1\right)\right], \tag{34}$$

and the down-crossing rate is given by

$$v_x^-(t,-b) = \frac{1}{\sqrt{2\pi}\sigma_x}\exp\left[-\frac{(-b-\mu_x)^2}{2\sigma_x^2}\right]\cdot\left[\frac{\sigma_y}{\sqrt{2\pi}}\exp\left(-\frac{\mu_{\tilde{y}}^2}{2\sigma_y^2}\right) + \frac{\mu_{\tilde{y}}}{2}\left(\operatorname{erf}\left(\frac{\mu_{\tilde{y}}}{\sqrt{2}\sigma_y}\right)-1\right)\right], \tag{35}$$

with

$$\mu_y = \mu_{\dot{x}} + \rho_{x\dot{x}}\frac{\sigma_{\dot{x}}}{\sigma_x}(b-\mu_x), \mu_{\tilde{y}} = \mu_{\dot{x}} + \rho_{x\dot{x}}\frac{\sigma_{\dot{x}}}{\sigma_x}(-b-\mu_x), \sigma_y = \sigma_{\dot{x}}\sqrt{1-\rho_{x\dot{x}}^2}, \tag{36}$$

By substituting Eqs. (34)–(35) into Eq. (30), and then incorporating the results into Eqs. (29), the time-dependent reliability, $L(t,b)$ of the base-isolation displacement can be evaluated.

4 Numerical exmaples

To verify the applicability of the proposed method, the ground motion illustrated in Fig. 1(a)–1(c) is adopted as a representative input, with its corresponding model parameters provided in Table 1. The system parameters associated with the considered BIS, as described by Eq. (10), are summarized in Table 2.

Table 2: Parameters of the base-isolation system.

m (kg)	c ($\mathrm{N\cdot s/m}$)	k (N/m)	α	A	β	γ	x_y (m)	F_y (N)
1.00×10^5	3.14×10^5	9.87×10^5	0.2	1	0.1	0.1	0.2	1.97×10^5

Subsequently, the stochastic displacement response of the BIS, obtained using the SLT-RKA method, is compared with the results from MCS based on 10,000 samples, as presented in Fig. 2(a) and Fig. 2(b).

As shown, the SLT-RKA method demonstrates excellent agreement with MCS results in terms of both the mean and standard deviation of the displacement response. These comparisons confirm the effectiveness and accuracy of the SLT-RKA method in capturing the key statistical characteristics of the stochastic structural response.

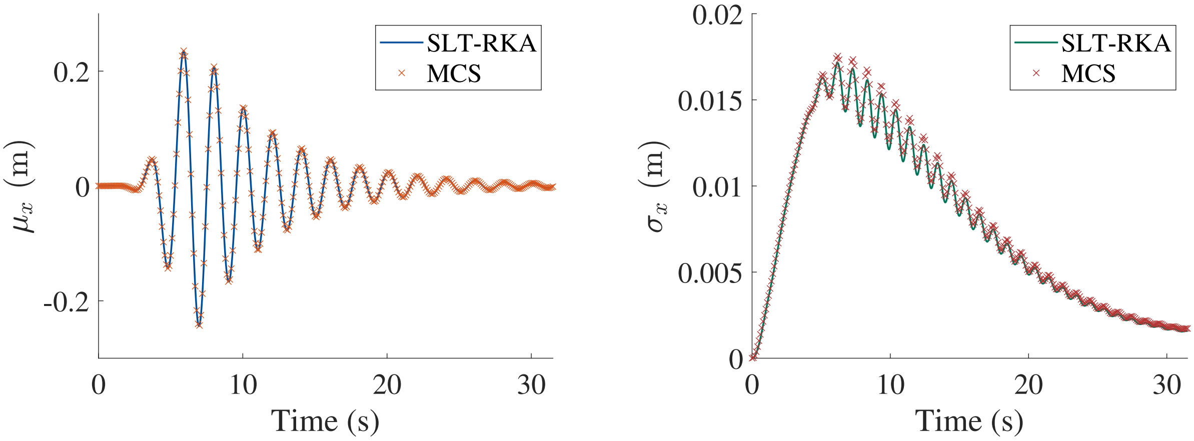

(a) (b)

Figure 2: (a) Mean and (b) standard deviation of the base-isolated displacement obtained using SLT-RKA and MCS.

To further assess the reliability prediction capability of the proposed method, various design thresholds b for the base-isolated displacement are considered. Specifically, four values of b are selected: $b = (0.25, 0.26, 0.27, 0.28)$ m. The reliability results obtained using the proposed method (denoted as “PM”) are compared with those from MCS in Fig. 3, and the relative errors are listed in Table 3.

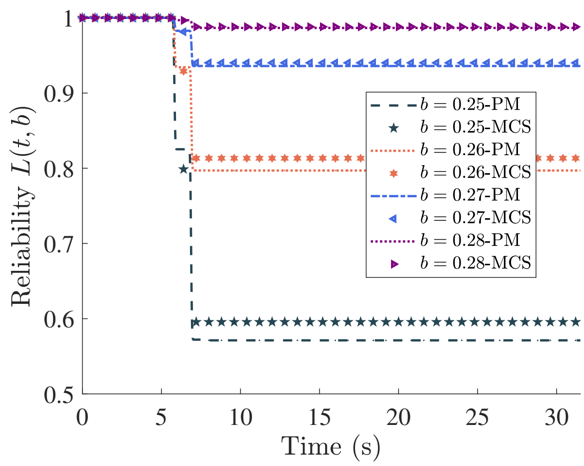

Figure 3: Time-variant reliability of the base-isolated displacement for different displacement limit values b.

Table 3: Comparison of reliability estimates for the base-isolated structure under stochastic pulse-like ground motions

$R_{b=0.30}$ (%)			$R_{b=0.31}$ (%)			$R_{b=0.32}$ (%)			$R_{b=0.33}$ (%)		
PM	MCS	Error	PM	MCS	Error	PM	MCS	Error	PM	MCS	Error
57.12	59.56	-4.10	79.70	81.33	-2.01	93.59	94.02	-0.45	98.66	98.81	-0.16

As shown in Fig (3) and Table 3, the proposed method exhibits excellent agreement with MCS results across all threshold levels, demonstrating its robustness and adaptability in reliability analysis. More importantly, the computational efficiency of SLT-RKA is remarkable: it requires only 1.91 seconds for the full reliability analysis, compared to 818.52 seconds required by MCS.

Despite the approximate nature of the proposed SLT-RKA method, which is based on assumptions such as Gaussian response distribution, equivalent linearization, and Poisson out-crossing modeling, the observed discrepancies with respect to MCS results remain limited and tend to diminish as the displacement limit increases. This trend aligns with the improved validity of the Poisson assumption in the tail region, where out-crossing events become increasingly rare and more independent. Given that the reliability level in the design of base-isolated structures should not be excessively low, the adopted assumptions are well-justified in practical applications.

Furthermore, the proposed method offers substantial computational advantages while maintaining acceptable accuracy, making it particularly suited for iterative reliability analyses in performance-based seismic design. The demonstrated balance between efficiency and precision underscores the applicability of the method to real-world engineering problems involving near-fault ground motions.

5 Conclusions

In this study an efficient semi-analytical method for evaluating the first-crossing probability of base-isolated structures subjected to stochastic pulse-like ground motions was developed. By modeling PLGMs as non-zero-mean random processes comprising a deterministic pulse component and a stochastic residual defined via its power spectral density, the proposed framework captures the essential characteristics of near-fault seismic excitations. The structural response, with also a non-zero-mean, is approximated using the SLT-RKA method, which combines statistical linearization with the Runge–Kutta algorithm to efficiently handle the nonlinear stochastic dynamics. A generalized expression for the decay rates of the time-varying mean response is further derived and incorporated into a Poisson-based out-crossing model to estimate first-crossing probabilities.

Through numerical examples, the proposed method is shown to exhibit excellent agreement with Monte Carlo simulation results across a wide range of displacement limit levels, confirming its accuracy and robustness. In addition, the significant reduction in computational time—achieving a speedup of over 400 times relative to conventional MCS—demonstrates its suitability for iterative reliability assessments. These findings highlight the potential of the proposed approach as a practical and computationally efficient tool for the performance-based seismic design and safety evaluation of base-isolated structures in near-fault regions.

REFERENCES

[1] R. S. Jangid, Optimum Damping in a Non-Linear Base Isolation System, Journal of Sound and Vibration 4 (189) (1996) 477–87.

[2] H. A. Jensen, D. S. Kusanovic, On the effect of near-field excitations on the reliability-based performance and design of base-isolated structures, Probabilistic Engineering Mechanics 36 (2014) 28–44.

[3] C. Providakis, Effect of LRB isolators and supplemental viscous dampers on seismic isolated buildings under near-fault excitations, Engineering Structures 30 (5) (2008) 1187–1198.

[4] J. W. Baker, Quantitative Classification of Near-Fault Ground Motions Using Wavelet Analysis, Bulletin of the Seismological Society of America 97 (5) (2007) 1486–1501.

[5] Y. Peng, R. Han, A comprehensive categorization method for identifying near-fault pulse-like ground motions, Earthquake Engineering & Structural Dynamics 53 (14) (2024) 4404–4431.

[6] G. P. Mavroeidis, A mathematical representation of near-fault ground motions, Bulletin of the Seismological Society of America 93 (3) (2003) 1099–1131.

[7] Y. Peng, C. Luo, C. Qiu, F. Kong, Stochastic simulation of velocity pulses of near-fault ground motions based on multivariate copula modeling, Probabilistic Engineering Mechanics 72 (2023) 103434.

[8] M. Dabaghi, A. Der Kiureghian, Stochastic model for simulation of near-fault ground motions: Stochastic Model for Simulation of Near-Fault Ground Motions, Earthquake Engng Struct. Dyn. 46 (6) (2017) 963–984.

[9] D. Yang, J. Zhou, A stochastic model and synthesis for near-fault impulsive ground motions, Earthquake Engineering & Structural Dynamics 44 (2) (2015) 243–264.

[10] G. G. Amiri, A. A. Rad, N. K. Hazaveh, Wavelet-Based Method for Generating Nonstationary Artificial Pulse-Like Near-Fault Ground Motions, Computer-Aided Civil and Infrastructure Engineering 29 (10) (2014) 758–770.

[11] G. W. Housner, Characteristics of strong-motion earthquakes, Bulletin of the Seismological Society of America 1 (37) (1947) 19–31.

[12] H. Tajimi, A statistical method of determining the maximum response of a building structure during an earthquake, 1960.

[13] R. Han, F. Kong, Y. Peng, Approximate analytical solution of non-zero-mean nonstationary response of MDOF hysteretic systems subject to pulse-like stochastic ground motions, Mechanical Systems and Signal Processing 221 (2024) 111742.

[14] J. He, A reliability approximation for structures subjected to non-stationary random excitation, Structural Safety 31 (4) (2009) 268–274.

[15] D. Thomson, Spectrum estimation and harmonic analysis, Proceedings of the IEEE 70 (9) (1982) 1055–1096.

[16] B. C. Lin, I. G. Tadjbakhsh, A. S. Papageorgiou, G. Ahmadi, Response of base-isolated buildings to random excitations described by the Clough-Penzien spectral model, Earthquake Engineering & Structural Dynamics 18 (1) (1989) 49–62.

[17] C. A. Martínez, O. Curadelli, M. E. Compagnoni, Optimal placement of nonlinear hysteretic dampers on planar structures under seismic excitation, Engineering Structures 65 (2014) 89–98.

[18] J. Dugundji, Envelopes and pre-envelopes of real waveforms, IEEE Transactions on Information Theory 4 (1) (1958) 53–57.

[19] B. K. Roy, S. Chakraborty, Robust optimum design of base isolation system in seismic vibration control of structures under random system parameters, Structural Safety 55 (2015) 49–59.

[20] E. H. Vanmarcke, On the Distribution of the First-Passage Time for Normal Stationary Random Processes, Journal of Applied Mechanics-Transactions of the ASME 42 (1) (1975) 215–220.

[21] S. O. Rice, Mathematical analysis of random noise, The Bell System Technical Journal 3 (23) (1944) 282–332.